

## Functionality of UPFC in Stability Improvement

S. V. Ravi Kumar and S. Siva Nagaraju  
 J.N.T.U.College of Engineering, Kakinada, A.P, India

**Abstract:** With increased power transfer, transient stability is increasingly important for secure operation. Transient stability evaluation of large scale power systems is an extremely intricate and highly non-linear problem. An important function of transient evaluation is to appraise the capability of the power system to withstand serious contingency in time, so that some emergencies or preventive control can be carried out to prevent system breakdown. In practical operations correct assessment of transient stability for given operating states is necessary and valuable for power system operation. Static VAR Compensator is a shunt connected FACTS devices and plays an important role as a stability aid for dynamic and transient disturbances in power systems. UPFC controller is another FACTS device which can be used to control active and reactive power flows in a transmission line. The damping of power system oscillations after a 3 phase fault is also analyzed with the analyzation of the effects of SVC and UPFC on transient stability performance of a power system. A general program for transient stability studies to incorporate FACTS devices is developed using modified partitioned solution approach. The modeling of SVC and UPFC for transient stability evaluation is studied and tested on a 10-Generator, 39-Bus, New England Test System.

**Key words:** Transient stability, SVC, UPFC, faults, critical clearing time, power system, VAR compensator

### INTRODUCTION

A power system is a complex network comprising of numerous generators, transmission lines, variety of loads and transformers. As a consequence of increasing power demand, some transmission lines are more loaded than was planned when they were built. With the increased loading of long transmission lines, the problem of transient stability after a major fault can become a transmission limiting factor (Mihalic *et al.*, 1996). Transient stability of a system refers to the stability when subjected to large disturbances such as faults and switching of lines (Padiyar, 2002). The resulting system response involves large excursions of generator rotor angles and is influenced by the nonlinear power angle relationship. Stability depends upon both the initial operating conditions of the system and the severity of the disturbance. The voltage stability and steady state and transient stabilities of a complex power system can be effectively improved by the use of FACTS devices (Igor and Peter, 2002).

SVC is a first generation FACTS device, can control voltage at the required bus thereby improving the voltage profile of the system. The primary task of an SVC is to maintain the voltage at a particular bus by means of reactive power compensation (obtained by varying the firing angle of the thyristors) (Hingorani and Gyugyi,

1999; Padiyar and Kulakarni, 1997). SVCs have been used for high performance steady state and transient voltage control compared with classical shunt compensation. SVCs are also used to dampen power swings, improve transient stability and reduce system losses by optimized reactive power control (Mithulananthan *et al.*, 2002). Representative of the third generation FACTS device is the Unified Power Flow Controller (UPFC) (Gyugi *et al.*, 1995). The UPFC consists of two voltage-sourced converters using Gate Turn Off thyristors (GTO), which operates from a common D.C. link. In this study dynamics of the system is compared with and without UPFC and SVC. Modeling of UPFC and SVC is carried out and the system stability is analyzed using the above FACTS devices. To achieve the optimum performance of FACTS controllers proper placement of these devices in the system is as important as an effective control strategy.

### MODELING OF POWER SYSTEM AND FACTS DEVICES (UPFC AND SVC)

**Synchronous machine model:** Mathematical models of a synchronous machine vary from elementary classical models to more detailed ones. In the detailed models, transient and sub transient phenomena are considered. Here, the transient models are used to represent the machines in the system, according to following equations.

To represent transient effects two rotor circuits, one field winding on the d-axis and a hypothetical coil (damper winding) on the q-axis are adequate.

$$T'_{do} * (dE'_q / dt) + E'_q = E_{fd} - (X_d - X'_d) i_d \quad (1)$$

$$T'_{qo} * (dE'_d / dt) + E'_d = (X_q - X'_q) i_q \quad (2)$$

Where

$T'_{do}$  is the d-axis open circuit transient time constant

$T'_{qo}$  is the q-axis open circuit transient time constant

$E'_{fd}$  is the field voltage

The rotor mechanical dynamics are represented by the swing equation:

$$2H * (dS_m / dt) = T_m - T_e - DS_m \quad (3)$$

$$(d\delta / dt) = S_m * \omega_b \quad (4)$$

Where  $S_m$  is slip,  $\omega_b$  is the base synchronous speed and  $D$  is the damping coefficient.

$T_m$  is the mechanical torque input and  $T_e$  is electrical torque output and is expressed as:

$$T_e = E'_q i_q + E'_d i_d + (X'_d - X'_q) i_d i_q \quad (5)$$

Stator transients are neglected and the stator reduces to simple impedance with reactance components in the d-axis and q-axis. The stator is represented by dependent current source  $I_G$  in parallel with the admittance  $Y_G$ . The equivalent circuit is shown in Fig. 1.

The  $Y_G$  and  $I_G$  are defined as:

$$Y_G = 1 / (R_a + jX'_d) \quad (6)$$

$$I_G = Y_G [E'_q + j(E'_d + E'_{dc})] e^{j\delta} \quad (7)$$

Where

$$E'_{dc} = (X'_d - X'_q) * i_q \quad (8)$$

The differential equation describing the effect of transient saliency is expressed as:

$$T_c * (d\Psi_c / dt) = [-\Psi_c - (X'_d - X'_q) i_q] \quad (9)$$

Where  $T_c$  is time constant of the dummy coil and  $\Psi_c$  is the voltage correction that accounts for the effect of transient saliency. Thus:

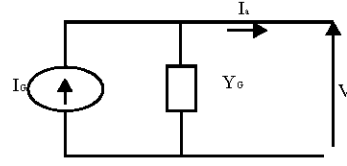


Fig. 1: Stator representation

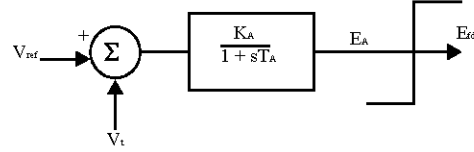


Fig. 2: AVR model

$$E'_{dc} = -\Psi_c \quad (10)$$

The generator armature current and terminal voltage in the q-d reference frame are related to their respective phasor quantities.

$$i_q + j i_d = I_a e^{-j\delta} \quad (11)$$

$$V_q + j V_d = V e^{-j\delta} \quad (12)$$

The angle  $\delta$  measures the rotor position of the generator relative to the synchronously rotating reference frame, which is implied in the phasor solutions of the network.

Referring to Fig.1, we have

$$I_a = I_G - Y_G V \quad (13)$$

Using Eq. 6, 7, 10, 11 and 12 Eq. 13 may be written as:

$$i_q + j i_d = \frac{[(E'_q + j(E'_d + E'_{dc})) - (V_q + j V_d)]}{R_a + jX'_d} \quad (14)$$

The generator terminal voltage is expressed as:

$$V_t = |V| = -\sqrt{(V_q^2 + V_d^2)} \quad (15)$$

**AVR model:** The voltage regulator configuration is shown in Fig. 2. The AVR equations are

$$T_A * (dE_A / dt) = -E_A + K_A (V_{ref} - V_t) \quad (16)$$

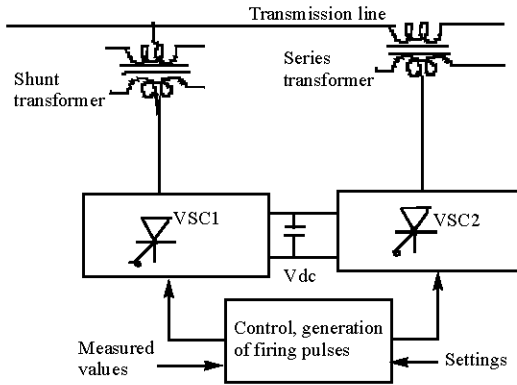


Fig. 3: General UPFC scheme

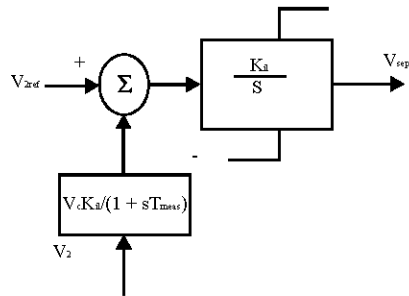


Fig. 4: Controller structure for  $V_{sep}$

$$\begin{aligned}
 E_{fd} &= E_A \cdot \text{if} \dots V_{rmin} < E_A < V_{rmax} \\
 &= V_{rmin} \cdot \text{if} \dots V_{rmin} > E_A \\
 &= V_{rmax} \cdot \text{if} \dots V_{rmax} < E_A
 \end{aligned}
 \tag{17}$$

**Unified Power Flow Controller (UPFC):** UPFC consists of two switching converters, which in the implementations considered are Voltage Sourced Converters (VSC) using Gate Turn-Off (GTO) thyristor valves, as illustrated in Fig. 3. These converters are operated from a common D.C. link provided by a D.C. storage capacitor. This arrangement functions as an ideal A.C. to A.C. power converter in which the real power can freely flow in either direction between the A.C. terminals of the two converters and each converter can independently generate (or absorb) reactive power at its own A.C. output terminal. In principle a UPFC can perform voltage support, power flow and dynamic stability improvement in one and the same device.

**Controller for  $V_{sep}$ :** The in phase component of the series injected voltage,  $V_{sep}$  is used to regulate the magnitude of the voltage  $V_2$ . The controller structure is shown in Fig. 4. In this  $V_{2ref}$  is the value of the desired magnitude of voltage  $V_2$  obtained from Eq. 18,  $T_{meas}$  is the constant to represent delay in measurements. A simple integral

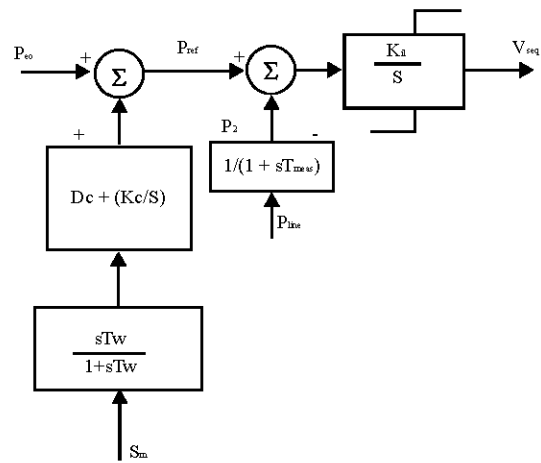


Fig. 5: Controller structure for  $V_{seq}$

controller is used for the control of  $V_{sep}$ . Limits are on the minimum and maximum values of  $V_{sep}$ . The gain of the integral controller has to be adjusted so as to prevent frequent hitting of the limits by the controller. It is also assumed that  $V_{sep}$  follows  $V_{sep}^{ref}$  without any time delay. During contingency  $V_{2ref}$  can itself be varied. The differential equations relating in-phase voltage control are

$$V_2 = V_R + jI_L X_R \tag{18}$$

$$\begin{aligned}
 \dot{V}_C &= (V_2 - V_C) / T_{meas} \\
 \dot{V}_{seq} &= K_{iL} (V_{2ref} - V_C)
 \end{aligned}
 \tag{19}$$

**Controller for  $V_{seq}$ :**  $V_{seq}$  is controlled to meet the real power demand in the line. The controller structure is shown in Fig. 5. Referring to Fig. 5,  $P_{eo}$  is the steady state power,  $D_c$  and  $K_c$  are constants to provide damping and synchronizing powers in the line,  $S_m$  is the generator slip,  $T_{meas}$  is the measurement delay and  $P_{line}$  is the actual power flowing in the line. It is assumed that  $V_{seq}$  follows  $V_{seq}^{ref}$  without any time delay.

It is necessary to distinguish between the roles of the UPFC as a power flow controller in order to achieve steady state objectives (slow control) and as a device to improve transient performance (requiring fast control). Thus, while real and reactive power references are set from the steady state load flow requirements, the real power reference can also be modulated to improve damping and transient stability. An auxiliary Signal ( $S_m$ ) is used to modulate the Power reference ( $P_{ref}$ ) of the UPFC. A washout circuit is provided so as to prevent any steady state bias. The differential equations relating quadrature voltage control are:

$$\dot{P}_2 = (P_{line} - P_2) / T_{meas} \quad (20)$$

$$\dot{V}_{seq} = K_{12}(P_{ref} - P_2) \quad (21)$$

**Modeling of UPFC for transient stability evaluation:** In two-port representation of UPFC, The current injections due to UPFC at the two ports are  $I_1$  and  $I_2$ , which have to be determined at every time step of the simulation process.

$$V_{se} = V_2 - V_1 \quad (22)$$

$$I_{sh} = I_1 + I_2 \quad (23)$$

It is to be noted that series injected voltage is sum of quadrature component and in phase components  $V_{seq}$  and  $V_{sep}$ . In a similar way, the shunt current is expressed as two components  $I_{shq}$  and  $I_{shp}$ . The magnitude of shunt real current is determined from real power balance requirement and is given by

$$I_{shp} = \text{Real}(V_{se} I_2^*) / V_1 \quad (24)$$

The magnitudes of the components of the series injected voltage,  $V_{sep}$  and  $V_{seq}$ . The network equation at the two ports of the UPFC, when the external network is represented by its Thevenin's equivalent at the two ports, can be written as:

$$\begin{bmatrix} V_{oc1} \\ V_{oc2} \end{bmatrix} = \begin{bmatrix} -Z_{eq} \end{bmatrix} \begin{bmatrix} I_1 \\ I_2 \end{bmatrix} + \begin{bmatrix} V_1 \\ V_2 \end{bmatrix} \quad (25)$$

Where  $V_{oc1}$  and  $V_{oc2}$  are the open circuit voltages across port1 and port2 respectively and  $Z_{eq}$  is the open circuit impedance (Thevenin's impedance) matrix of the external network at the two ports.

To solve the network equation  $I=YV$ , the current injections  $I_1$  and  $I_2$  have to be calculated where the UPFC is placed. Therefore the objective, when UPFC is incorporated in the transient stability algorithm, is to evaluate these current injections at those particular buses.

**Static Var Compensator (SVC):** Static var systems are applied by utilities in transmission applications for several purposes. The primary purpose is usually for rapid control of voltage at weak points in a network. Installations may be at the midpoint of transmission interconnections or at the line ends. Static var compensators are shunt connected static generators and or absorbers whose

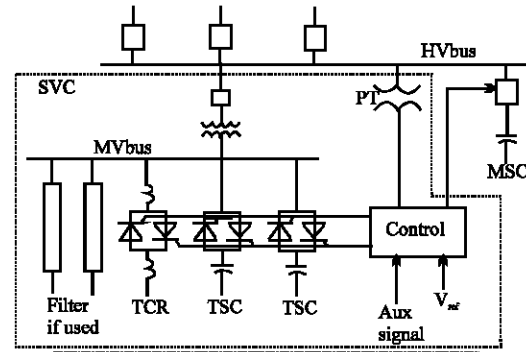


Fig. 6: Typical SVC system

outputs are varied so as to control voltage of the electric power systems. In its simple form SVC is connected of FC-TCR configuration as shown in Fig. 6. The SVC is connected to a coupling transformer that is connected directly to the ac bus whose voltage is to be regulated. The effective reactance of the FC-TCR is varied by firing angle control of the antiparallel thyristors. The firing angle can be controlled through a PI controller in such a way that the voltage bus where the SVC is connected is maintained at the reference value.

## DEVELOPMENT OF TRANSIENT STABILITY SOLUTION

Transient stability analysis is used to investigate the stability of power system under sudden and large disturbances and plays an important role in planning and operation of the power system. The transient stability analysis is performed by combining a solution of the algebraic equations describing the network with numerical solution of the differential equations. Although significant improvements have been made in the application of numerical and computational methods to the transient stability calculation, the computational demands are rising rapidly at the same time. Therefore there is a continual search for faster and accurate solutions to the transient stability problem.

**Partitioned-solution approach for transient stability equations:** The transient stability problem is defined by a set of non-linear Differential Equations (DAEs).

$$[\dot{Y}] = [f([Y],[X],t)] \quad (26)$$

$$0 = [g([y],[x])] \quad (27)$$

Equation 26 describes machine dynamics including their control circuits and Eq. 27 describes the network static behavior including steady state models of loads and algebraic equations of machines. The initial conditions are determined from a steady state power flow solution. The structure of Eq. 27 will change at certain instants of time due to fault initiation, fault clearing, etc. Such changes require re-solutions without advancing the time and produce discontinuous in the value of vector [x]. No discontinuity can appear in [y]. The differential equation set (1) is solved by integration separately for [y] and the algebraic set (27) is solved separately for [x]. Consider the step in numerical integration of (26) from a given point ((t<sub>n-1</sub>), [x (t<sub>n-1</sub>)] ) at time t<sub>n-1</sub>. The integration over the interval t<sub>n-1</sub> to t<sub>n</sub> to get [y(t<sub>n</sub>)], requires the corresponding value of a subset [u] of set of variables [x].

**Solution of power system equations:** A modified partitioned-solution method is developed here due to the programmable advantage compared to simultaneous solution approach. The set of differential equations describing the system is partitioned into three blocks and each block is solved separately. This approach leads to simple non-iterative and effective interfacing technique.

The DE s describing the system are separated into three groups.

(1) The des corresponding to the variables E<sub>q</sub>' , E<sub>d</sub>' , Ψ<sub>c</sub> whose dynamics are faster compared to δ and S<sub>mp</sub> are grouped together to form one set. This set defines the rotor electrical equations.

The rotor electrical equations are given as

$$\dot{E}'_q = \frac{1}{T'_{do}} [E_{fd} - (X'_d - X'_q) i_d - E'_q] \quad (28)$$

$$\dot{E}'_d = \frac{1}{T'_{qo}} [(X_q - X'_q) i_q - E'_d] \quad (29)$$

$$\dot{\Psi}'_c = \frac{1}{T_c} [-\Psi_c - (X'_d - X'_q) i_q] \quad (30)$$

From the synchronous generator model, the real and imaginary part of armature current is expressed as:

$$i_q + j i_d = \frac{[(E'_q + j(E'_d - \Psi_c))] - (V_q + jV_d)}{R_a + jX'_d} \quad (31)$$

Substituting for i<sub>q</sub> and i<sub>d</sub> using Eq. (31), the Eq. (28-30) can be grouped and expressed in the form

$$[\dot{Z}] = [A][Z] + [B][U] \quad (32)$$

The trapezoidal rule of integration is applied to solve the block 1:

$$[Z(t_n)] = [Z(t_{n-1})] + (\Delta t/2)[A][Z(t_n) + Z(t_{n-1})] + (\Delta t/2)[B][U(t_{n-1}) + U(t_n)] \quad (33)$$

$$[Z(t_n)] = [C_1][Z(t_{n-1})] + [C_2][U(t_{n-1})] + [C_3][U(t_n)] \quad (34)$$

Matrices [C<sub>1</sub>], [C<sub>2</sub>] and [C<sub>3</sub>] are defined as follows

$$[C_1] = [[U] - [A']^{-1}[[U] + [A']]] \quad (35)$$

$$[C_2] = [[U] - [A']^{-1}[B']] \quad (36)$$

It is important to note that for solution of the [z(t<sub>n</sub>)], the corresponding value of [u(t<sub>n</sub>)] is required.

(2) The des corresponding to the AVR forms Block II of the system DEs.

The differential equation representing the AVR is:

$$\dot{E}_A = (1/2)[-E_A + K_A(V_{ref} - V_t)] \quad (37)$$

After applying the trapezoidal rule of integration, Eq. 37 can be expressed as

$$E_A(t_n) = C_4 * E_A(t_{n-1}) + C_5 * V_t(t_{n-1}) + C_6 * V_t(t_n) + C_7 \quad (38)$$

Where

$$C_4 = [1 - (\Delta t/2T_A)]/[1 + (\Delta t/2T_A)]$$

$$C_5 = C_6 = -[(\Delta t/2) * (K_A/T_A)]/[1 + \Delta t/2T_A]$$

$$C_7 = [\Delta t K_A V_{ref}/T_A]/[1 + \Delta t/2T_A]$$

Once E<sub>A</sub>(t<sub>n</sub>) is obtained, E<sub>FD</sub>(t<sub>n</sub>) is easily obtained from conditions given in the Eq. 17. It follows from the Eq. 38 that calculation of E<sub>fd</sub>(t<sub>n</sub>) requires the corresponding value of V<sub>t</sub>(t<sub>n</sub>).

(3) Block III of the system DEs consists of the swing equations.

The equations representing the rotor dynamics are:

$$\dot{S}_m = \frac{1}{2H} [T_m - T_e - D * S_m] \quad (39)$$

$$\dot{\delta} = S_m * \omega_b \quad (40)$$

After applying the trapezoidal rule, the solution of Eq. 39 and 40 are expressed as:

$$S_m(t_n) = C_8 * S_m(t_{n-1}) + C_9 * T_e(t_{n-1}) + C_{10} * T_e(t_n) + C_{11} \quad (41)$$

$$\delta(t_n) = C_{12} * \delta(t_{n-1}) + C_{13} * S_m(t_{n-1}) + C_{14} * S_m(t_n) \quad (42)$$

Where

$$C_8 = \frac{4 * H - \Delta t * D}{4 * H + \Delta t * D}$$

$$C_9 = C_{10} = \frac{-\Delta t}{4H + \Delta t * D} \quad C_{11} = \frac{2 * \Delta t * T_m}{4H + \Delta t * D}$$

$$C_{12} = 1 \quad C_{13} = C_{14} = \Delta t \omega_b / 2$$

From Eq. 41, we see that only  $T_e(t_n)$  is required for the solution of  $S_m(t_n)$ . The calculation of the  $T_e(t_n)$  requires corresponding the values  $E_q'(t_n)$ ,  $E_d'(t_n)$ ,  $i_q(t_n)$  and  $i_d(t_n)$ . Once  $S_m(t_n)$  is available, the solution for the  $\delta(t_n)$  is straightforward as is seen in Eq. 42.

**Interfacing technique and overall solution procedure:**

The interfacing DEs and the network equation involves the prediction of the variables  $E_q'$ ,  $E_d'$ ,  $\Psi_c$ ,  $\delta$  so as to enable the calculation of  $I_G$ , which is required for the solution of the network.

A simple linear prediction defined by

$$\alpha(t_n)^{pred} = 2\alpha(t_{n-1}) - \alpha(t_{n-2}) \quad (43)$$

is used to predict the values of  $E_q'$ ,  $E_d'$ ,  $\Psi_c$ ,  $\delta$ ,  $t_{n-1}$ ,  $t_{n-2}$  are the previous two time-steps with respect to current time-step  $t_n$ . Thus the generator current injection estimated using the predicted values of  $E_q'$ ,  $E_d'$ ,  $\Psi_c$ ,  $\delta$  is

$$I_G(t_n)^{pred} = Y_G [E_q'(t_n)^{pred} + j(E_d'(t_n)^{pred} - \Psi_c(t_n)^{pred})] e^{j\delta(t_n)^{pred}} \quad (44)$$

In the essence  $I_G(t_n)^{pred}$  represents the interface between the DEs and network solution.

The solution procedure of the DAEs at the time step  $t_n$  is enumerated below:

Calculation of current injection vector  $[I(t_n)]$ .

All loads are modeled as constant impedance loads so  $[I_L] = 0$ , then only  $[I_G]$  has to be evaluated. Using Eq. 43, the predicted values of  $E_q'(t_n)^{pred}$ ,  $E_d'(t_n)^{pred}$ ,  $\Psi_c(t_n)^{pred}$  and  $\delta(t_n)^{pred}$  are obtained. Then  $I_G(t_n)^{pred}$  can be obtained

using Eq. 44. It may be noted that for the first time step of the solution, the predicted values of the variables are the same as the initial values.

- Solve the network equation

Having obtained  $I_G(t_n)$ , the network equation can now be solved to give the vector of the bus voltages  $[V(t_n)]$ .

- Solve the AVR equation

The  $V_t(t_n)$ , the generator terminal voltage, from step 2 is used to solve Eq. 37 and  $E_{fi}(t_n)$  follows easily.

- Solve the group of rotor electrical equations

Steps 2 and 3 yield the vector  $[u(t_n)]$  required to solve Eq. 34. Hence  $E_q'(t_n)^{pred}$ ,  $E_d'(t_n)^{pred}$  and  $\Psi_c(t_n)^{pred}$  are obtained. Calculate  $i_q(t_n)$  and  $i_d(t_n)$  and  $T_e(t_n)$  using Eq. 31 and 32, respectively.

- Solve the swing equations

Using  $T_e(t_n)$  calculated in step 4, Eq. 39 is solved to get  $S_m(t_n)$  which is then used in Eq. 40 to evaluate  $\delta(t_n)$ .

**TRANSIENT STABILITY EVALUATION WITH AND WITHOUT UPFC AND/OR SVC**

The transient stability program developed can take care of 3-phase symmetrical fault at a bus with an option of with line and without line outage. The stability of the system is observed with and without the UPFC.

**Solution steps:** The algorithm for the transient stability studies with FACTS devices involves the following steps:

1. Reads the line data. It includes the data for lines, transformers and shunt capacitors.
2. Form admittance matrix,  $Y_{BUS}$
3. Reads generator data ( $R_a, X_d, X_q, X_d', X_q', H, D$  etc).
4. Reads steady state bus data from the load flow results. ( $[V]$ ,  $[\delta]$ ,  $[P_{load}]$ ,  $[Q_{load}]$ ,  $[P_{gen}]$ ,  $[Q_{gen}]$ ).
5. Calculates the number of steps for different conditions such as fault existing time, line outage time before auto-reclosing, simulation time etc
6. Modify  $Y_{BUS}$  by adding the generator and load admittances.

For generator bus 'i'

$$Y_{ii} = Y_{ii} + Y_{gi} \quad Y_{gi} = \frac{1}{R_{gi} + jX_{di}}$$

For load bus 'i'

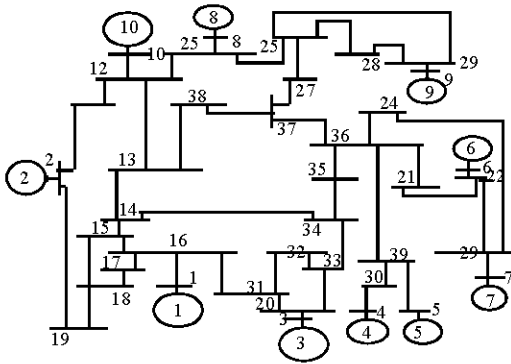


Fig. 7: 10-Generator, 39-Bus, new england test system

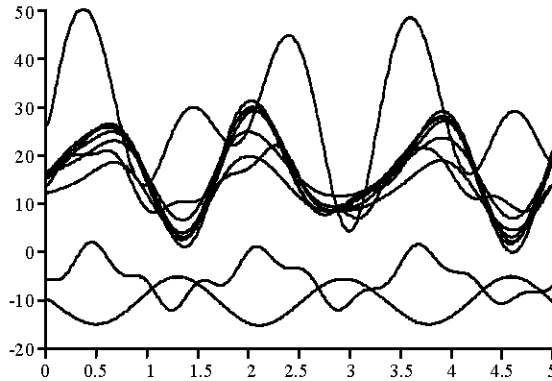


Fig. 8: Swing curves of generators #1 to #10

$$Y_{ii} = Y_{ii} + Y_{Li} \text{ where } Y_{Li} = \frac{P_{Li} + jQ_{Li}}{|V|^2}$$

7. Calculate fault impedance and modify the bus impedance matrix when there is any line outage following the fault.
8. Calculate the initial conditions and constants needed in solving the DAEs of generators, AVR etc.
9. Solves the network equation iteratively in each time step.
10. For  $X_r$ - $X_q$  models calculates  $V_d$ - $V_q$  using the obtained voltages and rotor angles.
11. Calculates the generator electric power outputs
12. The time step is advanced by the current time step.
13. Solves the generator swing equations using trapezoidal rule of integration keeping generator mechanical power output as constant.
14. Solves the AVR equations
15. Solves the UPFC and SVC. The bus current injection vector is modified with UPFC and SVC injection currents. Then network equation is again solved using  $[Y_{BUS}] [V]=[I_{inj}]$ .
16. Checks for number of steps.
17. Steps from 7-12 are repeated up to the total number of steps.
18. Plots the swing curves for all the generators

### CASE STUDY

Case studies are conducted, to evaluate the performance of the controller, on 10-Generator, 39-Bus, New England Test System (Fig. 7):

For this system, generator #9 is severely disturbed, so swing curves of generator #9 are only observed. Both Classical and Detailed models are considered for this study. A three-phase fault at any bus with a clearing time of 60 ms is considered to observe both transient stability and damping of power oscillations.

The following cases are considered

- Fault at bus #26, no line cleared, UPFC in line 29-26.
- Fault at bus #26, line cleared 26-28, UPFC in line 29-26
- Fault at bus #26, no line cleared, UPFC in line 15-14
- Fault at bus #26, no line cleared, UPFC in line 29-26 and SVC at 28 bus.
- Fault at bus #26, line cleared 26-28, UPFC in line 29-26 and SVC at 28 bus.
- Fault at bus #26, no line cleared, UPFC in line 15-14 and SVC at 28 bus.

### Generator:

$$X_d = 1.6, X_d' = 0.32, T_{d0}' = 6.0, X_q = 1.55, X_q' = 0.32, T_{q0}' = 0.44, H = 5.0, f_B = 60 \text{ Hz}$$

### Network:

$$X_r = 0.1, X_{L1} = X_{L2} = 0.2, X_b = 0.1$$

### AVR:

$$K_A = 200, T_A = 0.05, E_{fdmin} = -6.0, E_{fdmax} = 6.0$$

### Initial operating point:

$$V_g = 1.05, P_g = 0.75, E_0 = 1.0$$

### UPFC:

The limits on both  $V_{sep}$  and  $V_{seq} = 0.35$  pu.

The swing curves for all the ten generators represented by classical models are shown in Fig. 8. A three-phase symmetrical fault at bus 26 with a clearing time of 60 ms, for no line outage, is considered for the

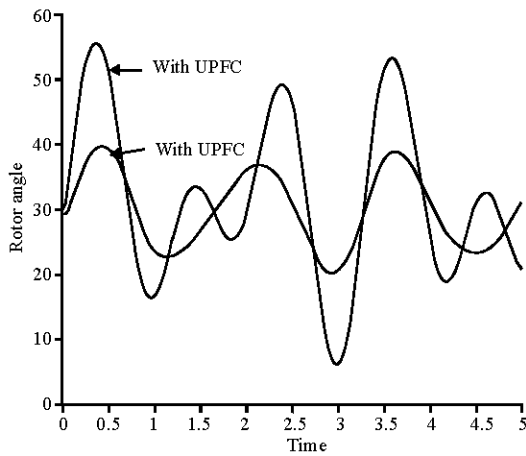


Fig. 9: Swing curves: Fault at bus#26, no line cleared, UPFC in line 26-29

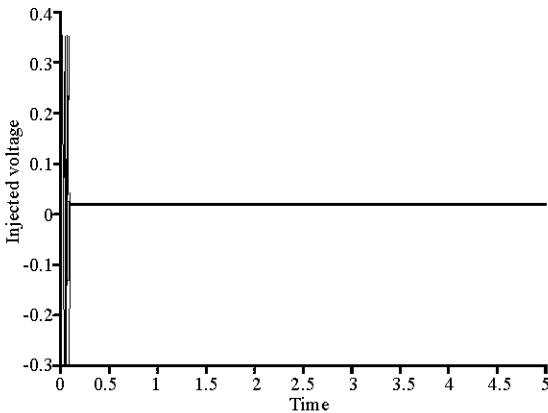


Fig. 10: Variation of  $V_{seq}$

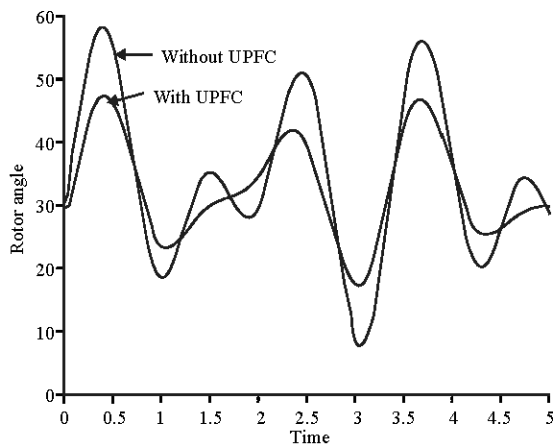


Fig. 11: Swing curves-Fault at bus#26, no line cleared, UPFC in line 14-15

study. It is observed from the Fig. 8 that only generator #9 is severely disturbed and so swing curves of

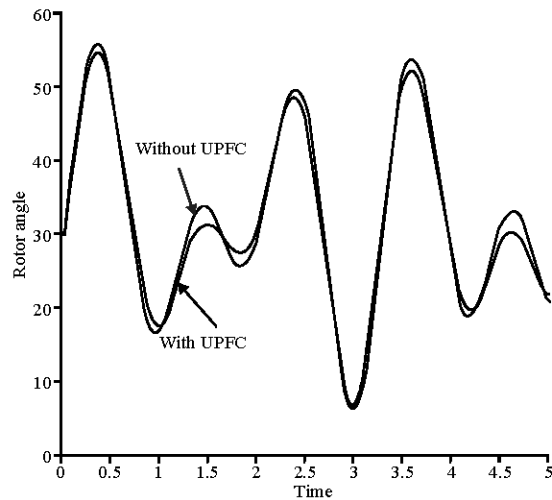


Fig. 12: Swing curves-Fault at bus #26, line cleared 26-28, UPFC in line 26-29

generator #9 are only considered for the investigation of the effect of UPFC on the system.

**Effect of UPFC's location:** For this case study, only control of  $V_{seq}$  is considered.  $V_{seq}$  is assumed to be zero at all instants. Hence, the UPFC behaves as a SSSC. The Fig. 9 shows the swing curves of generator #9 for case (i) with and without UPFC. In this case a three-phase fault at bus 26, which is cleared after three cycles without any line outage is considered. The UPFC is connected in the line 26-29, at the end of the line close to bus 26. Figure 9 shows the swing curve of generator 9, which separates from the rest of the generators when the system is unstable, for a fault at bus 26. Comparing the curves with and without the UPFC, it can be observed that the power controller helps in damping the power oscillations and also improves the transient stability by reducing the first swing. This is because in multi-machine systems there are many modes of oscillations and the control signal may not be effective in damping all the modes. Figure 10 shows the plot of the series injected voltage of the UPFC. UPFC is injecting leading voltage to damp oscillations. Several other cases are tested. It is observed that the effect of UPFC is more pronounced when it is placed near heavily disturbed generator rather than placed at remote location. This can be observed by comparing Fig. 9 and 12, where in Fig. 11 the swing curves shown for case (iii), in which UPFC is placed between lines 15-14. It is also observed that the effect of UPFC is more pronounced when the controller is placed near the faulted bus rather than placed at remote locations (Fig. 13-15).



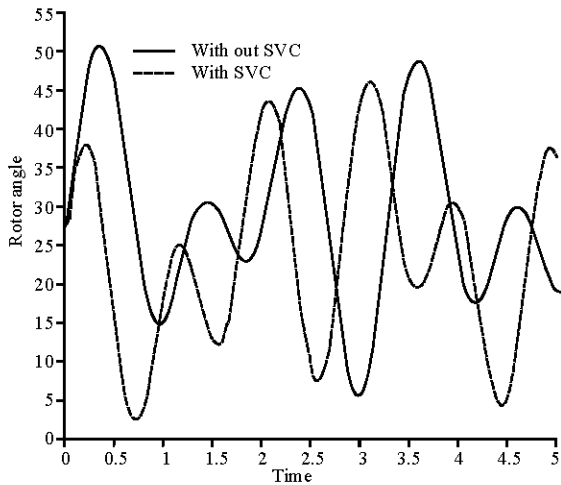


Fig. 13: Swing curves-Classical model: Fault at bus # 26, no line cleared, SVC at bus # 28

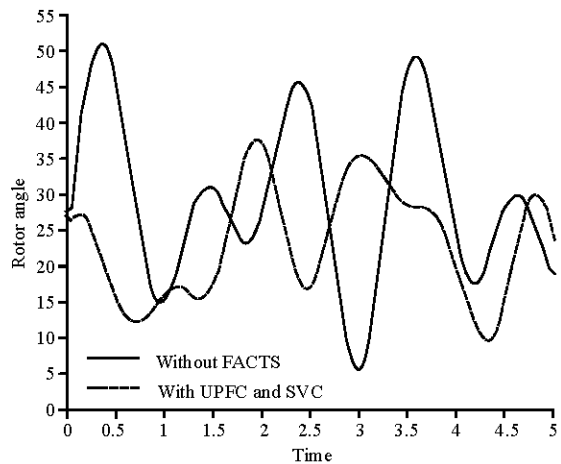


Fig. 14: Swing curves-Classical model: Fault at Bus # 26, no line cleared, UPFC in line # 26-29 and SVC at bus # 28

**Effect on critical clearing time with no line outage:** The effect of UPFC on transient stability of multi-machine system can be observed by observing critical clearing time ( $t_{cr}$ ). Table 1 and 2 gives critical clearing time for different cases and for different machine models.

From the tables it is observed that:

- The UPFC improves transient stability by improving critical clearing time
- Improvement in  $t_{cr}$  is more pronounced when the controllers are placed near the heavily disturbed generator.

**Comparison between AVR and UPFC:** To observe the effect of AVR consider test case (i). Detailed model has

Table 1: New England Test System: Fault at 26, Noline outage, UPFC is in line 29-26, closed to 29

Machine model	$t_{cr}$
1. Classical	
a. Without FACT devices	0.17 sec.
b. With UPFC	0.189 sec.
c. With SVC	0.26 sec
d. Combined control of SVC and UPFC	0.248 sec

Table 2: New England Test System: Fault at #26, line cleared 26-28 UPFC is in line 29-26, close to29

Transient stability curves	No line outage and line outage between 26 and 28
2. Classical	
a. Without FACT devices	
b. With UPFC	0.06 sec
c. With SVC	
d. Combined control of SVC and UPFC	

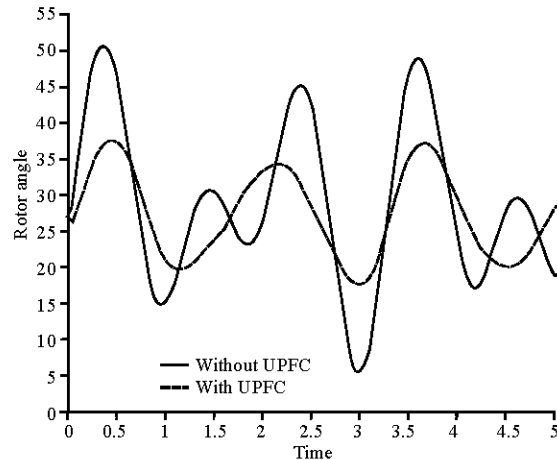


Fig. 15: Swing curves-classical model: Fault at bus # 26, no line cleared, UPFC in line # 26-29

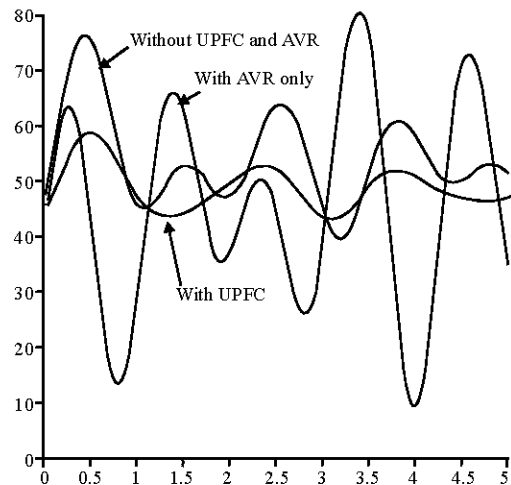


Fig. 16: Swing curves-detailed model: Fault at bus#26, no line cleared, UPFC in line 26-29

been considered here. Figure 16 shows swing curves for AVR-UPFC comparison.

From the Fig. 16, it can be observed that AVR improves transient stability by decreasing first swing, which is more pronounced compared to UPFC. But AVR introduces negative damping and the subsequent oscillations increasing as shown in the Fig. 16. With UPFC the oscillations are well damped out. It is, therefore, understood that UPFC has an edge over AVR when it comes to matter of damping oscillations.

### CONCLUSION

UPFC is modeled as dependent current injection model. Calculation of injected currents has been carried in such a way that it simplifies the inclusion of UPFC in generalized transient stability program. The transient stability and damping of power oscillations are evaluated with UPFC and SVC. Dynamics of the system is compared with and without presence of UPFC and SVC in the system. It is clear from the results that there is considerable improvement in the system performance with the presence of SVC and UPFC.

- The effect of UPFC is more pronounced when the controller is placed near heavily disturbed generator.
- The effect of UPFC is more pronounced when the controller is placed near faulted bus rather than placed at remote locations.
- UPFC helps in improving transient stability by improving critical clearing time.
- It is well known that AVR causes negative damping even though it improves transient stability. In this matter UPFC has an edge over this as it helps in damping oscillations.

- The transient stability is improved by decreasing first swing with UPFC and SVC.
- SVC helps in improving transient stability by improving critical clearing time

### REFERENCES

- Gyugyi, L., T.R. Rietman, A. Edris, C.D. Schauder, D.R. Torgerson and S.L. Williams, 1995. The Unified Power Flow Controller: A New Approach to Power Transmission Control, IEEE. Trans. Power Delivery, 10: 2.
- Hingorani, N.G. and L. Gyugyi, 1999. Understanding FACTS, IEEE Press.
- Igor Papic and Peter Zunko, 2002. Mathematical Model and Steady-State Operational Characteristics of a Unified Power Flow Controller, Electro technical Review, Slovenija, 69: 285-290.
- Mihalic, R., P. Zunko and D. Povh, 1996. Improvement of Transient Stability using Unified Power Flow Controller, IEEE. Trans. Power Delivery, 11: 485-491.
- Mithulananthan, N., Claudio A. Canizares, John Reeve and Graham J. Rogers, 2002. Comparison of PSS, SVC and STATCOM Controllers for Damping Power system Oscillations, IEEE. Transactions on Power System.
- Padiyar, K.R., 2002. Power System Dynamics: Stability and Control, (2nd Edn.), BS Publications, Hyderabad.
- Padiyar, K.R. and A.M. Kulakarni, 1997. Control Design and Simulation of Unified Power Flow Controller, IEEE. Trans. Power Delivery, pp: 1348-1354.